A Multiband Shunt Hybrid Active Filter with Sensorless Control

Surendra Kumar S[*] and Partha Sarathi Sensarma[†]

[*] Samsung India Software Operation Bangalore, 560093, India

[†] Department of Electrical Engineering, IIT Kanpur, U.P, 208016, India

ABSTRACT

This paper proposes a Multiband Shunt Hybrid Active Filter (SHAF) with sensorless control. A plant is modeled in the discrete- time domain and a controller is designed using the Pole shifting law in the polynomial domain. This control approach is very useful for filtering the load harmonics with reduced sensor counts where a low cost solution like SHAF is required. Multiple Synchronous Reference Frames (MSRF) and low pass filters are used to measure the 5th and 7th harmonic components separately from the load and filter currents. Individual current controllers are designed for the 5th and 7th harmonic currents. Control is realized in the stationary, three-phase (abc) reference frame. Performance of the controller is validated through simulation, using realistic plant and controller models, as well as experimentally on a full-scale distribution system.

Keywords: Multiband Shunt Hybrid Active Filter, Harmonic extraction, Multiple Synchronous Reference Frames, Poleshift controller

1. Introduction

Shunt Hybrid Active Filters (SHAF) consisting of an active filter and passive filters in series have been extensively reported in literature [1][2]. This combination is placed in shunt with a non-linear load, as shown in Fig. 1.

This topology overcomes the disadvantages of filter overload and system resonance with a passive filter. Also, it results in significant reduction in the active filter rating.

In its basic form, one SHAF branch can compensate for only one harmonic frequency. This requires multiple branches for each harmonic component in the load current.
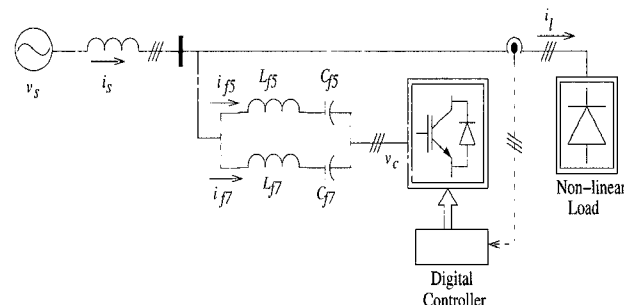

Fig. 1 Shunt Hybrid Active Filter

The possibility of using a single active filter in series with multiple passive filter branches has been reported [4]. The general circuit schematic of this approach is shown in Fig. 1. However, this approach uses a Proportional Integral (P-I) controller, which requires measurement of the filter capacitor voltages for feedforward compensation of disturbance and cross-coupling terms in the control law.

This requires additional complexity and adds to the cost of an otherwise low cost solution.

In this paper, a multiband SHAF is considered in which two passive filter branches, tuned at the 5th and 7th harmonic frequencies, are connected in series with the active filter. The switching harmonics of the active filter output are filtered by the passive filter impedance, which is inductive at the switching frequency. The plant is modeled in the discrete- time domain and a discrete-time control law is derived. The controller is designed using the Pole shifting law in the polynomial domain to radially shift the open loop system poles towards the origin i.e., more stable locations. With this Poleshift controller [5], sensing of capacitor voltages in the passive filter sections is not required. In order to damp filter resonances during transient changes in load harmonics, an active damping is introduced to greatly improve dynamic performance. Analytical control design is validated using simulation and experimental results on full-scale hardware. Multi-rate sampling is used to model the plant (fast sample-rate) and the controller (slow sample-rate). Switching of the active filter devices is considered though device losses are neglected.

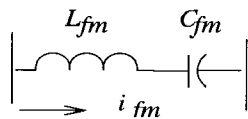## 2. Design of the passive filter

Fig. 2 Ideal Series Resonant Circuit

A series resonant filter circuit, is shown in Fig. 2. The filter impedance is given by,

$$Z_{fm}(s) = sL_{fm} + \frac{1}{sC_{fm}} = \frac{s^2 L_{fm} C_{fm} + 1}{sC_{fm}} \quad (1)$$

Resonant frequency, ω_m, of the filter is given by

$$\omega_m = \sqrt{\frac{1}{L_{fm} C_{fm}}} \quad (2)$$

where,

$$\omega_m = m..2\pi f \quad (3)$$

In this paper, as the 5th and 7th harmonic currents are to be compensated, m=5,7 and f=50Hz (fundamental frequency).

2.1 Selection of C_{fm}

The choice of C_{fm} is determined by the following factors. A high value reduces impedance at the fundamental frequency resulting in the passage of fundamental current, which is highly undesirable. Conversely, a low value results in a bulky inductor in the resonant branch, which in turn increases its cost. The optimal value of the filter capacitor is found to be 10 μF. Other filter parameters are mentioned in Table 1.

Table 1 Filter Parameters

L_{f5}	40.5mH
R_{f5}	1 Ω
C_{f5}	10μF
L_{f7}	20.7mH
R_{f7}	0.41 Ω
C_{f7}	10 μF

2.2 Impedance Characteristic of the Passive Filter Circuit

Fig. 3 shows the Bode plot (magnitude and phase) of the passive branch. It shows that the fundamental component and the switching harmonics (10 kHz or more) are blocked by the passive filter, whereas at the desired 5th and 7th harmonic frequencies the filter offers low impedance. The switching harmonics of the active filter output are filtered by the passive filter impedance, which gives more than 55dB attenuation at 10 kHz. Hence, only the required load harmonics will pass through these branches; fundamental and switching harmonics will be blocked. This results in a great reduction of the required rating of the Active filter.
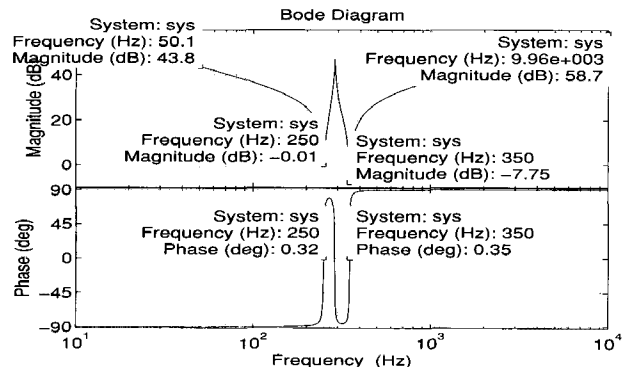

Fig. 3 Bode Magnitude plot for $Z_f(s)$

3. System Model

The state space model of the SHAF system for the 5th and 7th harmonic currents is given by

$$\frac{d}{dt}\begin{bmatrix} i_{fm} \\ v_{fm} \end{bmatrix} = \begin{bmatrix} \dfrac{-R_{fm}}{L_{fm}} & \dfrac{-1}{L_{fm}} \\ \dfrac{1}{C_{fm}} & 0 \end{bmatrix}\begin{bmatrix} i_{fm} \\ v_{fm} \end{bmatrix} + \begin{bmatrix} \dfrac{-1}{L_{fm}} \\ 0 \end{bmatrix} v_{cm} \quad (4)$$

$$y = \begin{bmatrix} 1 & 0 \end{bmatrix}\begin{bmatrix} i_{fm} & v_{fm} \end{bmatrix}^T$$

where, m =5, 7.

From (4) the transfer function between filter currents and control voltage is

$$G_{pm}(s) = \frac{I_{fm}(s)}{V_{cm}(s)} = \frac{-s/L_{fm}}{s^2 + \left(R_{fm}/L_{fm}\right)s + 1/L_{fm}C_{fm}} \quad (5)$$

4. Harmonic Extraction

In this paper, only the 5th and 7th harmonic components are measured for compensation. These are extracted from a measurement of the load current using Multiple Synchronous Reference Frames (MSRF) and low pass filters [3],[4]. Phase locking with the fundamental component of the PCC voltage is achieved through a PLL [6]. Denoting the fundamental phase angle as θ, transformations for each of the rotating reference frames are carried out as shown in Fig. 4.
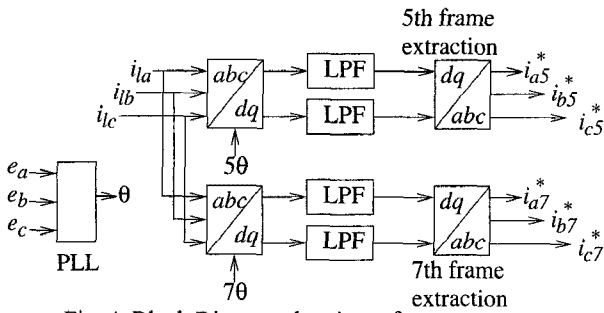

Fig. 4 Block Diagram showing reference current generation using MSRF

5. Current Controller Design

Individual current controllers are designed for the 5th and 7th harmonic currents. The harmonic currents,

extracted above, are used as reference commands for the individual current control loops. Control is realized in the stationary, three-phase (abc) reference frame.

5.1 Controller for the mth harmonic current

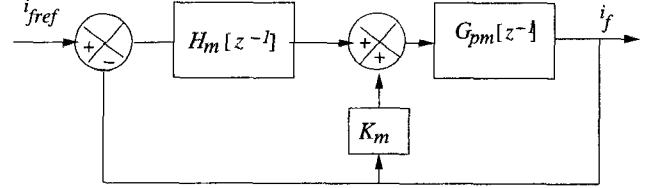The closed-loop model of the system is shown in Fig. 5.

Fig. 5 Closed Loop current controller schematic

$G_{pm}(z)$ is the discrete-time (z-domain) transfer function of the plant and $H(z)$ denotes the Pole shift controller. Since control is realized using a digital processor, it is appropriate to transform the plant transfer function into its discrete-time equivalent. The zero-order-hold equivalent of the plant is obtained using the following transformation [7].

$$G_{pm}(z) = (z-1)Z\left\{\frac{G_{pm}(s)}{s}\right\} \quad (6)$$

Consequently, the discrete-time plant transfer function is determined as

$$G_{pm}(z^{-1}) = \frac{B_m(z^{-1})}{A_m(z^{-1})} = \frac{b_{m1}z^{-1} + b_{m2}z^{-2}}{1 + a_{m1}z^{-1} + a_{m2}z^{-2}} \quad (7)$$

Expressing the controller transfer function $H(z)$ as

$$H_m(z^{-1}) = \frac{S_m(z^{-1})}{R_m(z^{-1})} = \frac{s_{m0} + s_{m1}z^{-1}}{1 + r_{m1}z^{-1}} \quad (8)$$

From Fig. 5, the closed loop system transfer function is

$$i_{fm}[k] = \frac{B_m(z^{-1})S_m(z^{-1})}{A_m(z^{-1})R_m(z^{-1}) + B_m(z^{-1})S_m(z^{-1})} i_{frefm}[k] \quad (9)$$

The controller parameters are obtained from the solution of the following Diophantine equation.

$$A_m(z^{-1})R_m(z^{-1}) + B_m(z^{-1})S_m(z^{-1}) = T_m(z^{-1}) \quad (10)$$

In (10) $T_m(z^{-1})$ is the closed loop system characteristic equation obtained after shifting the open loop poles. It is chosen to be of the following form

$$T_m(z^{-1}) = A_m(\lambda z^{-1}) = 1 + \lambda a_{m1} z^{-1} + \lambda^2 a_{m2} z^{-2} \quad (11)$$

where, λ ($0 < \lambda < 1$) is the Pole shift factor and determines the proximity of the closed-loop poles to the origin. A larger value of λ implies the closed loop poles are close to the open loop pole locations. As smaller values of λ require a larger control effort, for the SHAF system, this implies a higher output voltage demand from the active filter. However, this would increase the VA rating of the active filter and would, therefore, undermine the cost advantage of SHAF. So, the Pole shift factor is chosen here to be 0.8. Using this advanced control method, source harmonic currents are reduced below the limits prescribed in IEEE 519-1992, even with distorted PCC voltages. The system parameters are listed in Table 2.

Table 2 System parameters

Sampling interval(T_s)	100 μs
Switching frequency (f_c)	10kHz
Load inductance (L_d)	10mH
Load resistance (R_d)	30 Ω
PCC voltage (l-l, rms)	415 V
DC bus voltage (V_{dc})	80 V

Solving (10) and (11), the numerator and denominator polynomials of the 5th and 7th harmonic current controllers are obtained as listed in Tables 3 and 4.

Table 3 5th harmonic current controller

System num poly	b_{51}=-0.0025, b_{52}=0.0025
System den poly	a_{51}=-1.9729, a52=0.997
Controller num poly	s_{50}=-374.2825, s_{51}=320.7645
Controller den poly	r_{51}=0.7892
Closed loop poles	0.981+0.137i, 0.981-0.137i, -0.803

Table 4 7th harmonic current controller

System num poly	B_{71}=-0.0048, b_{72}=0.004
System den poly	a_{71}=-1.95, a_{72}=0.998
Controller num poly	s_{70}=-184.06, s_{71}=162.42
Controller den poly	r_{71}=0.789
Closed loop poles	0.974+0.193i, 0.974-0.193i, -0.792

5.2 Active Damping

The quality factor for 5th harmonic filter is

$$Q_{f5} = \frac{\omega_5 L_{f5}}{R_{f5}} = 63.5 \quad (12)$$

In order to damp filter resonances during transient changes in load harmonics, Q_{f5} has to be reduced. For this, series resistance of the 5th harmonic filter has to be increased, but adding physical resistance would increase losses. Instead, a ''virtual resistance'' [8] is added which is essentially an active damping term introduced in the control law and is given as

$$u_1 = H_m(z-1)i_{frefm} - i_{fm}$$
$$u = u_1 + K_m i_{fm} \quad (13)$$

where K_m is the virtual resistance and u is the control input.

5.3 Composite Controller

Using the above design procedure for the two controllers, analytical predictions of the closed-loop performance are reported here. The w-plane plots are analyzed to obtain the phase error (between reference command and output) for the 5th and 7th harmonic currents. Fig. 6 shows the magnitude and phase plot in the w-plane for the 5th harmonic controller, after transformation [7] of (9) to the w-plane, using

$$w = \frac{2}{T_s} \frac{z-1}{z+1} \quad (14)$$

From Fig. 6, the predicted phase error for the 5th harmonic current is negligible (approximately 1.7°). The corresponding plot for the 7th harmonic controller is also obtained in a similar fashion. Fig. 7 shows the magnitude and phase plot in the w-plane for the 7th harmonic controller. From Fig. 7, the predicted phase error for the 7th harmonic current is also found to be negligible (approximately 2.0°).

6. Simulation Results

The performance of the closed loop system is simulated for both pure sinusoidal and distorted PCC voltage cases.

The active filter is simulated using ideal switches so as to include switching action without considering switching losses. A multi-rate simulation is carried out using a 2 μs sampling interval for the continuous time plant and 100 μs for the discrete-time controller. The system parameters used are indicated in Tables 1 and 2. The performance of the MSHAF is tested under various operating conditions. Specifically, the performance under distorted PCC voltages and de-tuning of the passive filter are investigated and reported.

Fig. 8 shows the simulated results for pure sinusoidal PCC voltage. Fig. 9 shows the FFT analysis of the source and load currents. In this, the 5th and 7th source harmonic currents are reduced within IEEE 519-1992 limits and the 11th and 13th source harmonic currents are not affected.
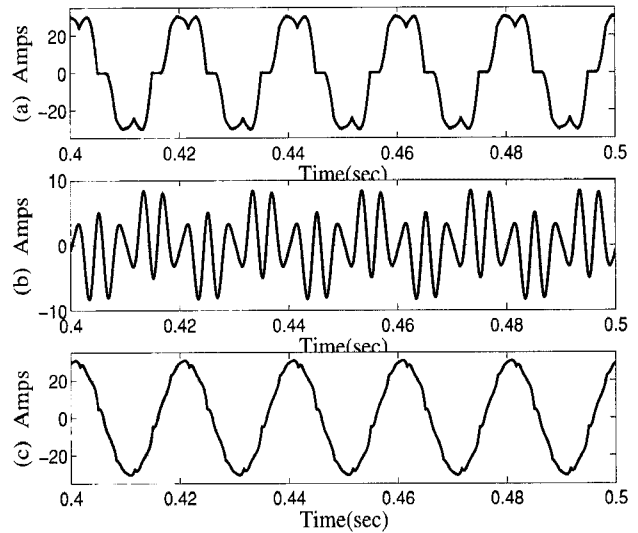

Fig. 8   Case A: (a) Load current; (b) Filter current;
(c) Source current
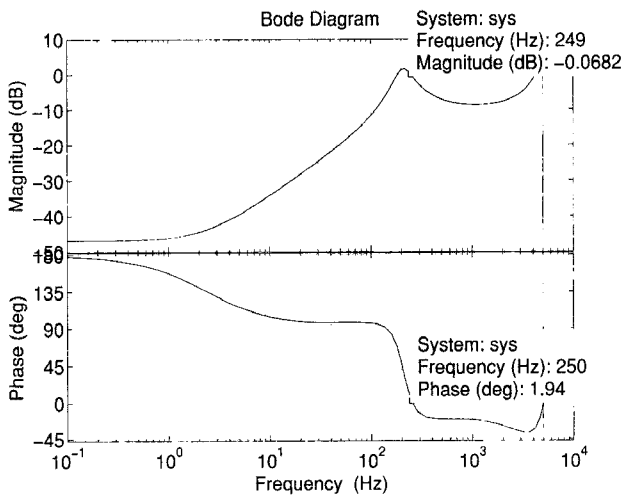
Fig. 6   Magnitude bode plot (w-plane) of closed loop system

6.1 PCC voltage without distortion
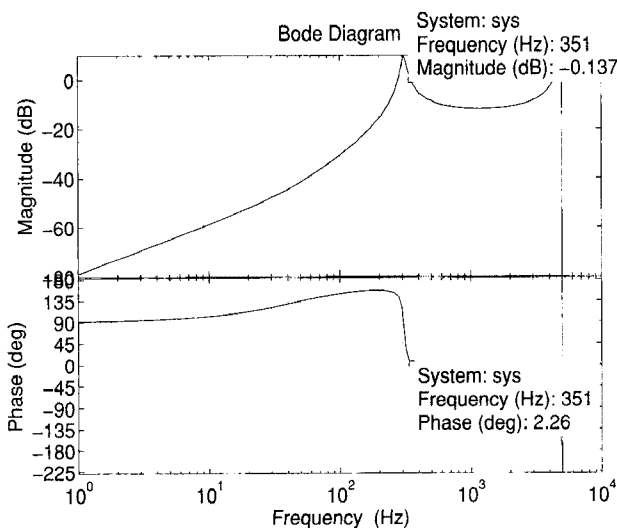
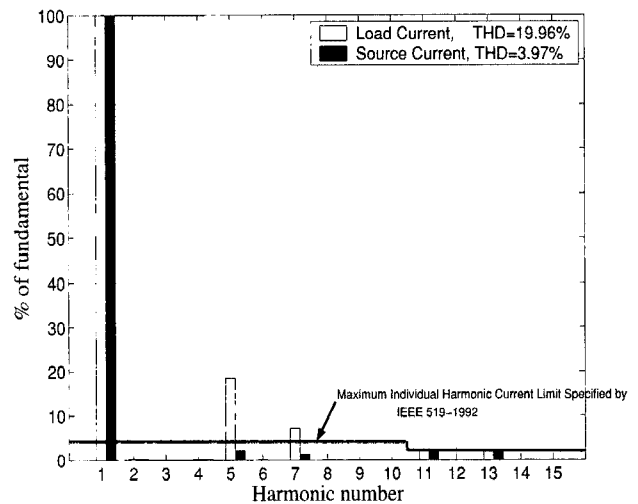Fig. 7   Magnitude bode plot (w-plane) of closed loop system

Fig. 9   Case A: FFT Comparison of Load and Source currents

6.2   PCC voltage with distortion

Fig. 10 shows the simulated results for distorted PCC voltage having 5% of the 5th and 4% of the 7th harmonics. Fig. 11 shows the FFT analysis of the source and load currents. In this, the 5th and 7th source harmonic currents

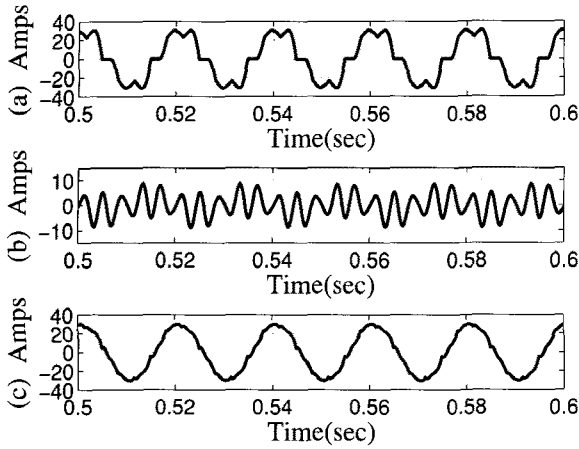are reduced within IEEE 519-1992 limits and the 11th and 13th source harmonic currents are not affected.

Fig. 10 Case B: (a) Load current; (b) Filter current; (c) Source current

Fig. 11 Case B: FFT Comparison of Load and Source currents

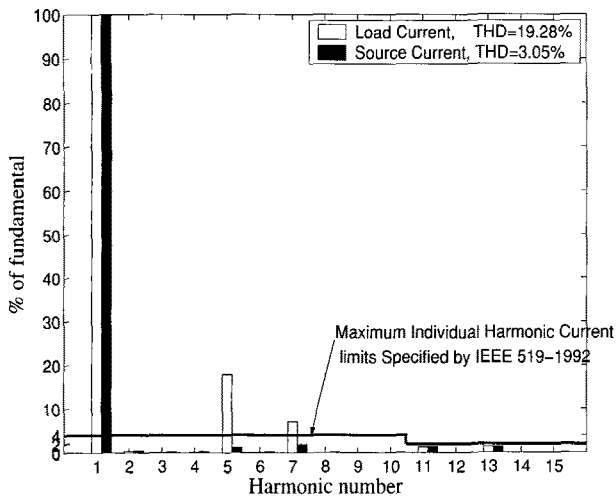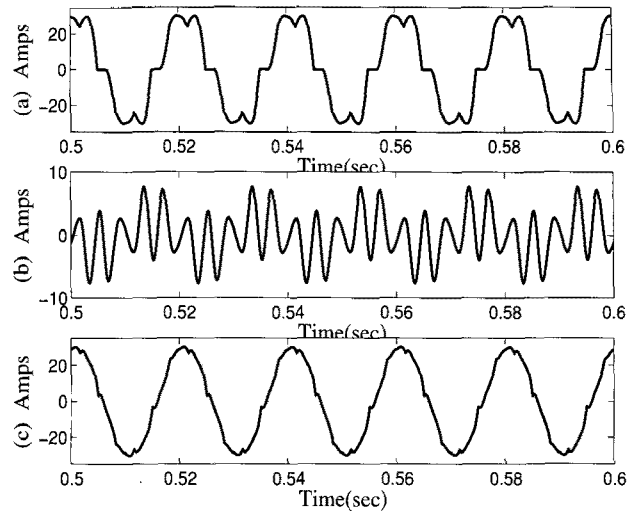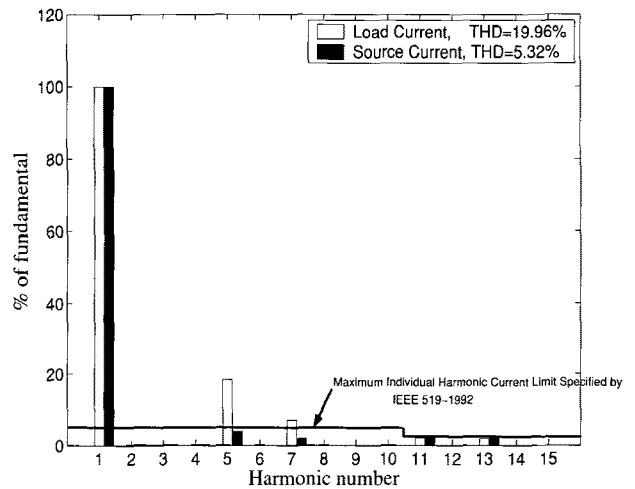Fig. 12 Case C: (a) Filter current; (b) Load current; (c) Source current

Fig. 13 Case C: FFT Comparison of Load and Source currents

6.3 De-tuned passive filter

Fig. 12 shows the simulated results for +5% De-tuned 5th and 7th harmonics LC components. This has shifted the corner frequency of the 5th harmonic filter from 250 Hz to 238 Hz. For the 7th harmonic filter the shift is from 350 Hz to 332 Hz.

Fig. 13 shows the FFT analysis of the source and load currents. In this, the 5th (3.92%) and 7th (1.93%) source harmonic currents are reduced within IEEE 519-1992 limits and the 11th and 13th source harmonic currents are not affected.

7. Experimental Results

The Pole shift control strategy was experimentally tested on a 415 V, 3-phase, 50 Hz distribution line. The load comprised a diode rectifier feeding a resistive load through an inductive filter. A two-level, low power (400 VA) inverter (active filter) was used. The passive filter parameters used are listed in Table 1. The entire control algorithm including harmonic extraction and PLL was realized on a DSP platform, using TMS320F240 processor. Hall effect current sensors were used to sense the filter and load currents. As a three-wire system was considered, only two line currents were sensed.

The active filter was designed along with all associated protection and gate triggering circuitry. Sensed signals were sent to the on board ADC and the PWM signals having a carrier frequency of 10 kHz were generated using the Simple compare unit of the DSP. In the experiment, the inverter DC bus voltage was held constant with the help of a diode bridge rectifier.

The experimental test setup is shown in Fig. 14. Using this set-up, the performance of the MSHAF was tested under different rectifier loading conditions. Due to practical constraints, neither arbitrary distortion in the available PCC voltage nor de-tuning of the passive filter could be created.
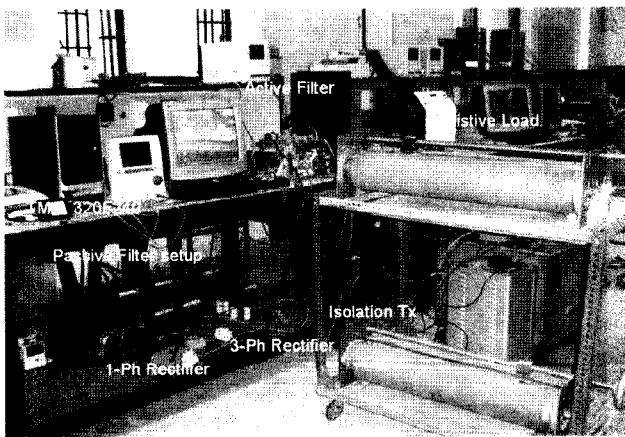

Fig. 14 MSHAF Experimental test setup

Fig. 15 shows a particular case where the fundamental component of the load current is 6 A (rms). The filter current, load current and source current waveforms are shown. The source current waveforms are seen to be practically sinusoidal.
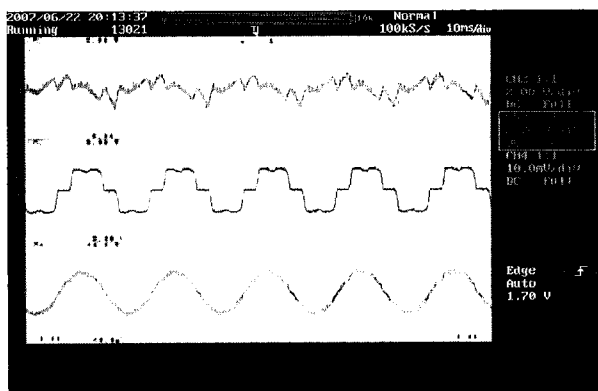

Fig. 15 (a)Filter current ; (b)Load current ; (c)Source current
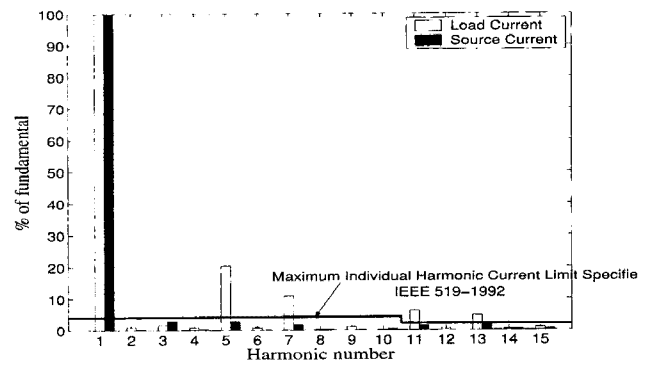

Fig. 16 FFT Comparison of Load and Source currents

Fig. 16 shows the FFT analysis of the source and load currents. In this the 5th (2.44%) and 7th (1.57%) source harmonic currents are reduced within IEEE 519-1992 limits and the 11th and 13th source harmonic currents are reduced by a small amount. This is, however, purely incidental as the control does not focus on compensation of these harmonics.
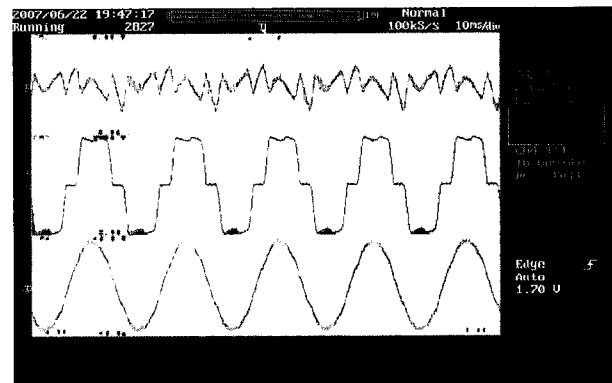

Fig. 17 (a) Filter current (b) Load current (c) Source current

Fig. 17 shows the results for another loading condition. Here the load current (fundamental, rms) is 12 A.
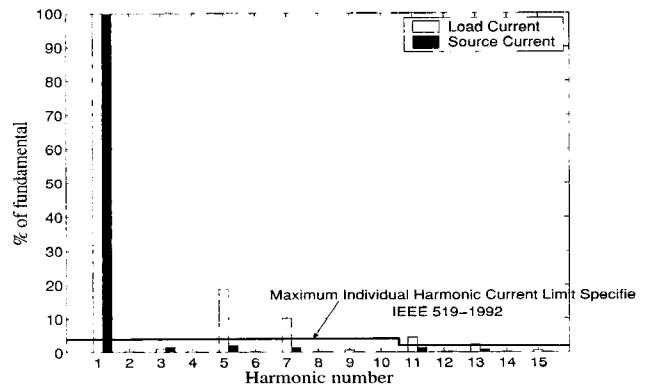

Fig. 18 FFT Comparison of Load and Source currents

Fig. 18 shows the FFT analysis of the source and load currents. Also, in this case, the 5th (2.24%) and 7th (1.07%) source harmonic currents are reduced within IEEE 519-1992 limits.

8. Conclusion

A Multiband SHAF scheme with a Pole shift controller is shown to be an attractive realization approach for harmonic compensation. Using this advanced control method, harmonics in the source current are controlled within limits specified by IEEE 519-1992. Use of a reduced sensor count along with an active damping scheme ensures a low cost solution without sacrificing any performance advantage. The complete analytical design procedure of the controller parameters is presented. It is verified by simulation that the proposed approach is immune to parameter variations in the passive filter and distortions in the supply voltage. The Pole shift control algorithm for the 5th and 7th harmonics was verified experimentally on a full-scale diode rectifier load operating in a 3-phase, 415 V, 50 Hz system. The DC bus voltage of the hybrid active filter was supported by a small rating diode rectifier. The experimental results obtained completely validate the analytical and simulation results.

References

[1] Fujita. H., Akagi. H., "A practical approach to harmonic compensation in power systems-series connection of passive and active filters", *IEEE Transactions on Industry Applications*, Vol. 27, No. 6, pp. 1020-1025, Nov/Dec. 1991.

[2] Po-Tai Cheng, Bhattacharya. S, Divan. D. M., "Line Harmonics Reduction in High-Power Systems Using Square-Wave Inverters Based Dominant Harmonic Active Filter", *IEEE Transactions on Power Electronics*, Vol. 14, No. 2, pp. 265-272, March 1999.

[3] Bhattacharya. S., Divan. D. M., Banerjee. B., "Synchronous Reference Frame Harmonic Isolator Using series Active Filter", *Proc. 4th EPE*, Vol. 3, pp. 30-35, 1991.

[4] Sukin Park, Soo-Bin Han, Bong-Man Jung, Soo-Hyun Choi, Hak-Geun Jeong, "A Current Control Scheme Based on Multiple Synchronous Reference Frame for Parallel Hybrid Active Filter", *Power Electronics and Motion control conference 2000*, Proceedings PIMEC 2000. The Thrid International, Beijing, China, Aug. 2000.

[5] Ghosh. A., Jindal. A. K., Joshi. A., "Inverter control using output feedback for power compensating devices", *IEEE Region 10 Conference on Convergent Technologies for Asia-Pacific Region*, TENCON 2003, Bangalore, India, Oct. 2003.

[6] Kaura. V, Blasko. V., "Operation of phase locked loopsystem under distorted utility conditions", *IEEE Transactions on Industry Applications*, Vol. 33, No. 1, pp. 58-63, Jan/Feb. 1997.

[7] B.C. Kuo, Digital Control Systems, Mc-Graw Hill, 1999.

[8] Pekik Argo Dahono, "A Control Method to Damp Oscillation in the input LC filter of AC-DC PWM Converters", *IEEE Power Electronics Specialists Conference*, PESC 2002, Queensland, Australia, June 2002.

Surendra Kumar S was born in Nellore, India in 1980. He received the B.Tech degree from JNTU College of Engineering, Kakinada, India and M.Tech degree in Electrical Engineering from IIT Kanpur, India, in 2005 and 2007, respectively. Since 2007, he has been with Samsung India Software Operations, Bangalore India as a Senior Software Engineer. His areas of interest are Power Electronics, Control Systems and Telecommunications.

Partha Sarathi Sensarma received his B.E.E ('90), M.Tech ('92) and PhD (2001) from Jadavpur University, Kolkata, India, Indian Institute of Technology, Kharagpur and Indian Institute of Science, Bangalore, respectively. He had previously worked with the Motor Design Department of Bharat Bijlee Ltd., Thane, India and in a thermal power plant of CESC Ltd., Kolkata, India. From Oct 2000 till June 2002, he was with the Power Electronics Department of ABB Corporate Research at Baden-Daettwil, Switzerland. Since July 2002, he has been with the Department of Electrical Engineering, I.I.T Kanpur, India, as an Assistant Professor. His research interests are in the areas of Power Quality, Renewable Energy Delivery, Motor Drives and Power Supplies.